東京大学大学院新領域創成科学研究科
社会文化環境学専攻

2022 年度
修　士　論　文

Detecting Dangerous Cycling Behaviors with Inertial Measurement Unit
慣性計測ユニットを使用した危険な自転車運転の検出

2022 年 07 月 15 日 提出
指導教員　瀬崎　薫　教授

董　学甫
Dong, Xuefu

Contents

List of Figures

List of Tables

Chapter 1

Introduction

1.1 Background

Single-handed riding behavior is omnipresent, usually transient, but always jeopardizing (Fig. 1.1). It threatens every road user with surged risk of bicyclist-involved crushes. The global annual death toll of cyclists is estimated to reach 40 thousand [1]. Improper maneuvering behaviors are a key contributing factor behind this unacceptably high number. For instance, engaging in distracting secondary tasks during cycling is shockingly prevalent [2] and contributes to driver error, sometimes resulting in tragedies [3].

Single-handed cycling weakens riding balance and delays braking responses, and the cognitive load of smartphone operations exacerbates the mental burden of cyclists and undermines their visual sensitivity to roadside objects [4]. In Japan, inappropriate steering caused an average of 1,500 bike-involved accidents each year in the 2010s [5]. Accident numbers are expected to climb higher with fast-growing markets for bike-sharing and bike-based food delivery services. Tradi-

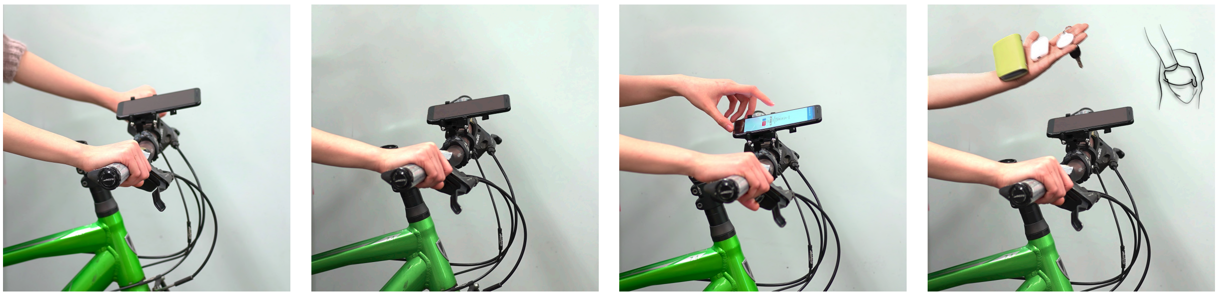

Figure 1.1 Illustration of cycling behaviors in our scope (from left): Normal, Hand-Drop, Phone-Tab, Take-from-Pocket

tional efforts to mitigate traffic hazard has their own limitation, which usually includes legislation, infrastructure plan, and manufacture design. Research has suggested that impulsive distracted behavior of cyclists is not likely to reduce by legislation alone[6]. On the other hand, the advanced driver assistance system (ADAS) has been introduced to automobiles, which efficiently enables collision avoidance instrumental collision avoidance systems. Nonetheless, cyclists could expect the above vehicle-born systems to be neither installed on most motor vehicles nor on their own bicycles, since ADAS usually require expensive LiDAR and camera sensors, along with the power supply and computing resources. These facts highlight the need for a ubiquitous, real-time method of safety-checking single-handed cycling.

Modern smartphones have versatile functions, such as environmental sensors, data processors, and instant feedback. These rich functions allow human activity recognition technologies to be deployed to smartphones without any additional devices. For example, based on the function, numerous smart safeguard solutions for automobiles [7, 8] and micro-mobility vehicles [9] have been proposed. These studies suggest that using smartphone functions can encourage cycling safety. However, the detection of single-handed cycling has not yet been addressed. Collecting single-handed riding events using a smartphone will allow the provision of numerous services to prevent dangerous riding in the future data-enhanced mobility society. The crucial challenges that we aimed to address are detailed below:

Subtle Difference Extraction: Empirically, The differences between the movement pattern of single-handed cycling and that of two-handed cycling may be neglectable. Biomechanics research [10] indicates that upper limbs contribute no more than 2.5% to the output work of the crank, which concurs to comments from some experiment participants. It is challenging for our model to extract representatives that are sensitive to hand-drop-caused movement pattern change from motion signals mixed with noises from terrain and normal maneuver changes.

Constrained Data Collection: We have to build a user-independent method since we cannot ask new users to perform dangerous single-handed cycling for personalization. Moreover, as the status quo, we cannot find any public data resources concerning single-handed cycling. In our own experiment, the experiment volume of dangerous cycling behavior has to be compressed, which makes the feature extraction more challenging.

Adaptability and Robustness: A key point for practicable cycling inspection is the reliability with complex terrains and across user-dimension. Thereby our system needs to extract the coherence in both-hand and single-handed cycling scenarios and be adaptive to common urban road surfaces such as asphalt road and pavement.

1.2 The Objective and Method of this Study

In this study, we propose DoubleCheck, a single-handed cycling detection method. Our proposed method predicts `double-handed` and `single-handed` cycling conditions using smartphone-embedded motion sensors using a vector autoregressive (VAR) machine-learning model and a wavelet scattering network. Our demonstrably effective approach (§ 3.2.3) collects time-frequency-domain features via lightweight computing from input motion data. We evaluated the performance of the proposed method using motion data from 22 participants during bicycle riding on two road surfaces. The resultant F1-score of 0.97 for the accuracy of determining cycling hand(s) and 0.69 for distraction recognition validate DoubleCheck' s practical safety-checking capability (§ 4).

The contributions of this work are summarized as follows:

- A method for single-handed cycling monitoring using a smartphone
- A feature extraction scheme using the wavelet scattering network and vector autoregression model
- A model performance evaluation and recommended future directions

Chapter 2

Related Works

With the spread of micro-mobility vehicles (e.g., bicycles), research promoting their operational safety has been increasingly performed. These studies used built-in cameras, motion sensors, and microprocessor units of smartphones and wearable devices to detect unsafe behaviors during bicycle operations [11, 12, 13]. These ubiquitous devices have the potential to provide a common safety-alerting platform for bicyclists worldwide. In this section, we summarize related studies about single-hand bike-riding detection from the viewpoint of handlebar grip recognition, cyclist monitoring, and environmental detection using embedded mobile sensors.

2.0.1 Handlebar Grip Detection

It is simple to leverage embedded tactile sensors or dynamometers to detect whether the cyclist is holding the bicycle handlebar. Such sensors have been demonstrably effective in kinematic research [14, 15, 16]. Nevertheless, their simple implementation makes them susceptible to tampering and cheating in real-life situations. Dancu et al. produced the Gesture Bike [17], which leverages a depth camera mounted at the front of the bike. Bonilla et al. [18] employed two gyroscope-embedded wearable devices for similar purposes. Unfortunately, these techniques require cyclists to equip their bikes with expensive instruments or to wear at least one smartwatch in bicycling or driving [19], which is less prevalent than navigation smartphones.

2.0.2 Bicyclist Maneuver Monitoring

Bicycle steering monitoring has long attracted attention in the field of human-computer interaction research. The scope of such research consists of maneuvering dynamics, physiological data [20], and body gestures. Our work follows this stream and is inspired by extant work in this field. For example, Miah et al. [21] proposed an accuracy-augmented positioning algorithm based on the fusion of sensors and models. This work highlighted the bike's specific low-dimensions-of-freedom kinetic properties, which aided our feasibility analysis (3.1). [22] leveraged a handlebar-borne smartphone to build a method of tracking basic braking and turning behaviors. Usami et al. [23] refined this idea with better recall in turning recognition by employing noise cancellation and feature extraction techniques. While only regular maneuvers were concerned in the above works, BikeMate [24] is most similar to our work. It took a step forward towards a more complex scope of standing pedaling, retrograde riding, and lane-weaving. Their framework demonstrates the capability of the smartphone to monitor evident actions with individual-level characteristics, meanwhile subtler ones such as single-handed cycling remain unexplored.

2.0.3 Bicycling Surrounding Detection

External-oriented systems can handle the fast-changing traffic contexts faced by cyclists while supporting real-time environmental adaptability for smart cycling. In particular, they detect geographic information composed of traffic dynamics, terrain conditions [25], air quality, etc. Many related tools are supported by data crowdsourcing to provide services without prior knowledge [26]. A collaborative geographic enrichment structure developed by Verstockt et al. [27] automatically annotates road and terrain taxonomies based on gathered-on-the-ride motion recordings and position data, enabling geographic web services. Bil et al. [28] introduced a dynamic comfort index of cycling routes, achieving a strong correlation coefficient of -0.94 via subjective evaluations. BikeL [29] can sense and visualize street-light statuses using a smartphone ambient light sensor. CycleGuard [30] leverages an acoustic-based approach to detect and warn of potential right-hook collisions. Our work inherits the lessons learned from these detection capabilities to extend the service to multiple road surfaces.

In contrast to the aforementioned works, we envision a long-lasting background service that recognizes bicyclist steering behaviors while detecting surrounding road conditions to deter single-handed cycling. The input to DoubleCheck comprises merely simple IMU motion readings, avoiding usage of battery-draining GNSS sensors and web service communications and processing.

Chapter 3

Detection Method for Single-Handed Riding Using Smartphone

3.1 Motivation & Feasibility Study

Single-handed cycling behaviors can help model successive errors that cause crashes and near-crashes [31]. Examples of single-handed cycling include tapping a smartphone mounted on the handlebar (*Phone-Tap*), taking something out of one's pocket (*Take-from-Pocket*), or taking a hand off the handlebars for resting (*Hand-Drop*). See Fig. 1.1.

Research has suggested that impulsive distracted behavior of cyclists is not likely to be reduced by legislation alone, and effective strategies include constraining proximate characteristics such as constraining phone accessibility[6]. Granted, existing research has proposed systems that monitor the motion of bicycles and their operators using dedicated tools and/or wearable devices. However, even with these systems, the detection of single-handed cycling has not yet been realized, and there are major restrictions on suitable equipment and installation locations.

If we could collect single-handed cycling event data, the information could be used to provide just-in-time suggestions for preventing dangerous cycling behaviors. Moreover, the suggestion could be refined with a detailed categorization of single-handed cycling. For example, there is no doubt that the alert for *Phone-Tap* should be more imperative than that for *Hand-Drop*. Similarly, left-handed cycling should be warned more intensely than right-handed cycling for those right-handed people. Therefore, the objective of this research is to propose a single-handed cycling detection method that satisfies the following requirements:

- **Hand Detection:** The exact cycling hand(s) must be automatically detected on different road profiles.

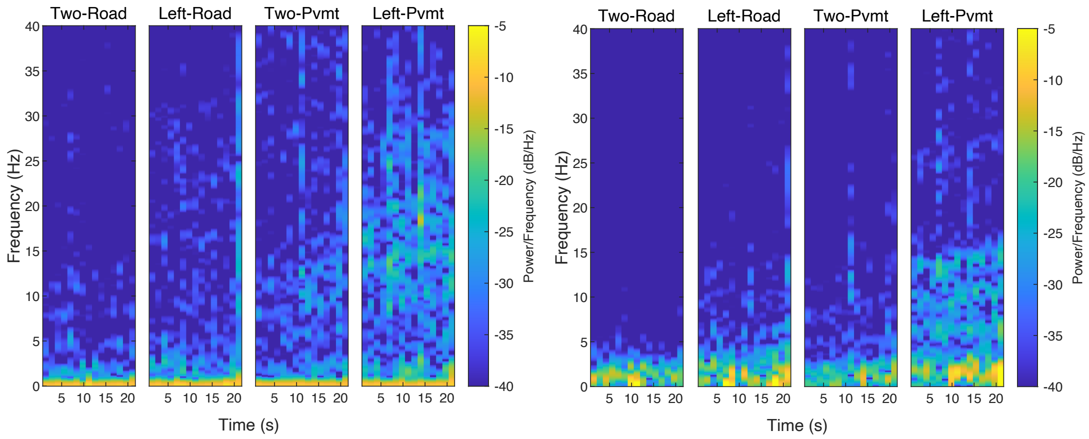

(a) X axis of acceleration (b) Z axis of angular velocity

Figure 3.1 Spectrogram of motion signals for double- and single-handed cycling on road and pavement.

- **Distraction Recognition:** Types of single-handed cycling must accurately reflect ground-truth cyclist behaviors.
- **Practicability:** The capability is restricted to the built-in IMU sensor of an off-the-shelf smartphone for real-time detection and classification of single-handed cycling.

3.1.1 Mechanics of Single-Handed Cycling

The handlebar hand grip is one of the three points of physical contact between a cyclist and the bicycle being operated. Although the upper limbs have little to do with crank-power output, they help stabilize bicycle direction and balance via the trunk and back muscles and the contralateral arm muscles [32]. The peak force applied to a handlebar can exceed 70 Newtons under normal cycling conditions [33]. Therefore, it is reasonable to infer that handlebar control is jeopardized when one of the two anchors (hands) is removed. Moreover, biomechanical studies have proven that altering the hand position on bend handlebars coincides with changes in major body positions during cycling [34]. Specifically, reaching down to grasp the lower drop-bar causes a 77% greater anterior pelvic tilt angle and an 11% greater trunk flexion angle than when grasping the top flat bar [35]. Meanwhile, the top limit of pressure on the seat could shrink by more than 20% (same crank capacity for both hand positions) [36]. This implies that a cyclist engaging in potentially distracting and unbalanced behaviors based on diverse hand trajectories may easily lead to unique motion patterns in the bike, including the handlebars.

3.1.2 Motion Data from Single-Handed Cycling

For an initial investigation of the capacity of motion sensors in commodity smartphones, we asked one male volunteer who was proficient in cycling to perform two-handed and left-handed cycling on roads and pavements for about 100 m, respectively, with a smartphone (Google Pixel 3a) in the handlebar mount. Because stability is most noticeable in lateral movement and yaw rotations (owing to the limited kinematics of cycling [21]), we illustrate the spectrum of motion data along the two axes in Fig. 3.1, from which two observations were drawn: 1) under the same road conditions, the acceleration signal of left-handed cycling tends to enjoy denser power than the two-handed mode over 15 Hertz, and so does the angular speed signal over 5 Hz. Similar patterns are found in our comparison between cycling on roads and pavements; 2) the power increment of left-handed cycling is much more evident on pavements than on roads. The profile developed from this test supports the feasibility of detecting single-handed cycling and road profiles simultaneously, and it corroborates the dangers of unbalanced single-handed cycling, regardless of proficiency.

3.2 System Design

In this study, we proposed an approach for detecting single-handed cycling detection, called DoubleCheck. Our method uses motion sensors on an off-the-shelf smartphone with machine learning. The scope of single-handed events in this study includes four types of cycling behaviors: two-handed cycling and three types of single-handed cycling. Note that we choose to utilize IMU signals rather than a screen-touch event for *Phone-Tap* to make our method more practical. Because smartphone applications are usually prohibited to listen to touch events in other applications. In addition, from our scope, we exclude other common single-handed cycling activities, such as, holding an umbrella and reaching for bottles, due to their unaffordable risk in our experiment.

Figure 3.2 presents DoubleCheck' s basic design, including the three steps used to estimate whether the rider is single-hand cycling. In the first step, DoubleCheck collects motion data from an off-the-shelf smartphone (see Section 3.2.1). In the second step, the raw data collected from the motion sensor are smoothed, sliced, and streamed into the AR model and the wavelet scattering network for the *data processing* step. Section 3.2.2 describes the data preprocessing method, and Section 3.2.3 presents our method of discovering the vibration patterns of cycling based on the two extracted features from time and frequency domains. Then, during the *detection* step (see Section 3.2.4), a support vector machine (SVM) classifier is trained to identify the road surfaces and the exact hand(s) being used for bike steering. If a single-hand cycling event is detected, the module further estimates the activity of the spare hand. We realized our method by MATLAB.

3.2.1 Data Collection

To build a classification model using supervised machine learning for single-handed cycling, we prepared labeled motion data for single- and double-handed cycling. To compile the dataset, we assembled a test bike mounted with an off-the-shelf smartphone (Google Pixel-3a equipped with Android 11 OS), a capacitive touch sensor (SKU-6515 [37]) and a cycling log camera (VR-220 [38]).

The test bike is presented in Fig. 3.3. To accumulate motion data, DoubleCheck collected acceleration and gyroscope data from the smartphone mounted to the handlebar. The smartphone was marginally inclined horizontally along the roll and yaw axes for more discrete measurements. The DoubleCheck application was created using Flutter and the Dart language, and the collected sensor data were saved into a local comma-separated value (CSV) file.

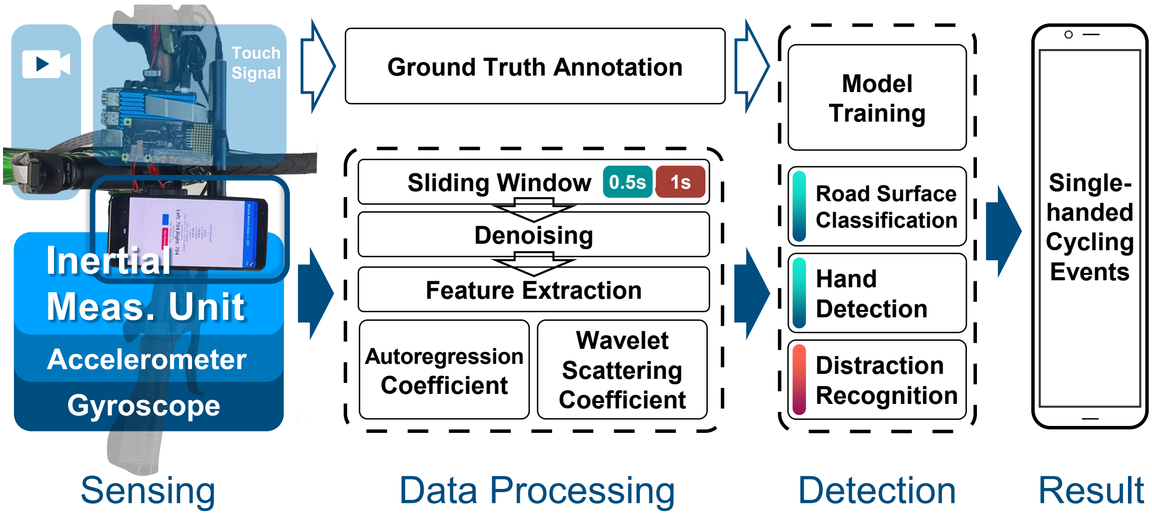

Figure 3.2 DoubleCheck workflow.

The Raspberry Pi-controlled tactile sensor collected ground-truth gripping events. It was connected to copper wires buried in the handlebar. The Raspberry Pi (RPi) program was written in Python3 and partially derived from the Bare Conductive Library. The ground-truth acquisition procedure is illustrated in Fig. 3.3. The touch status was recognized by capacitance readings from the tactile sensor and validated by watching cycling log videos. During cycling, the touch data and motion readings were continuously collected by the RPi, transmitted to the smartphone via a mobile hotspot, and stored in CSV-format files. The sample rate of all sensors was 80 Hz. Additionally, the RPi recorded 60-fps cycling log videos with millisecond timestamps for post hoc analysis.

3.2.2 Pre-processing

The raw motion readings contained intrinsic noise from the hardware, as well as acute disturbances from road surfaces. Thus, we first smoothed the data with a Hempel filter, a moving median filter that replaces the outliers with the local median. Here, an outlier is defined as a value of more than k times the local deviation away from the local median in a length-l window. These settings were made empirically ($l = 13$ and $k = 9$) to allow for the precise removal of disturbances. We then sliced the data using the sliding-window method with different lengths. The hand-detection window size was 40 samples (0.5 s), and the distraction-recognition window comprised 80 samples. A 20-sample-length overlap was implemented in both situations. Usually, there is a trade-off that longer sliding window size with more information would result in greater

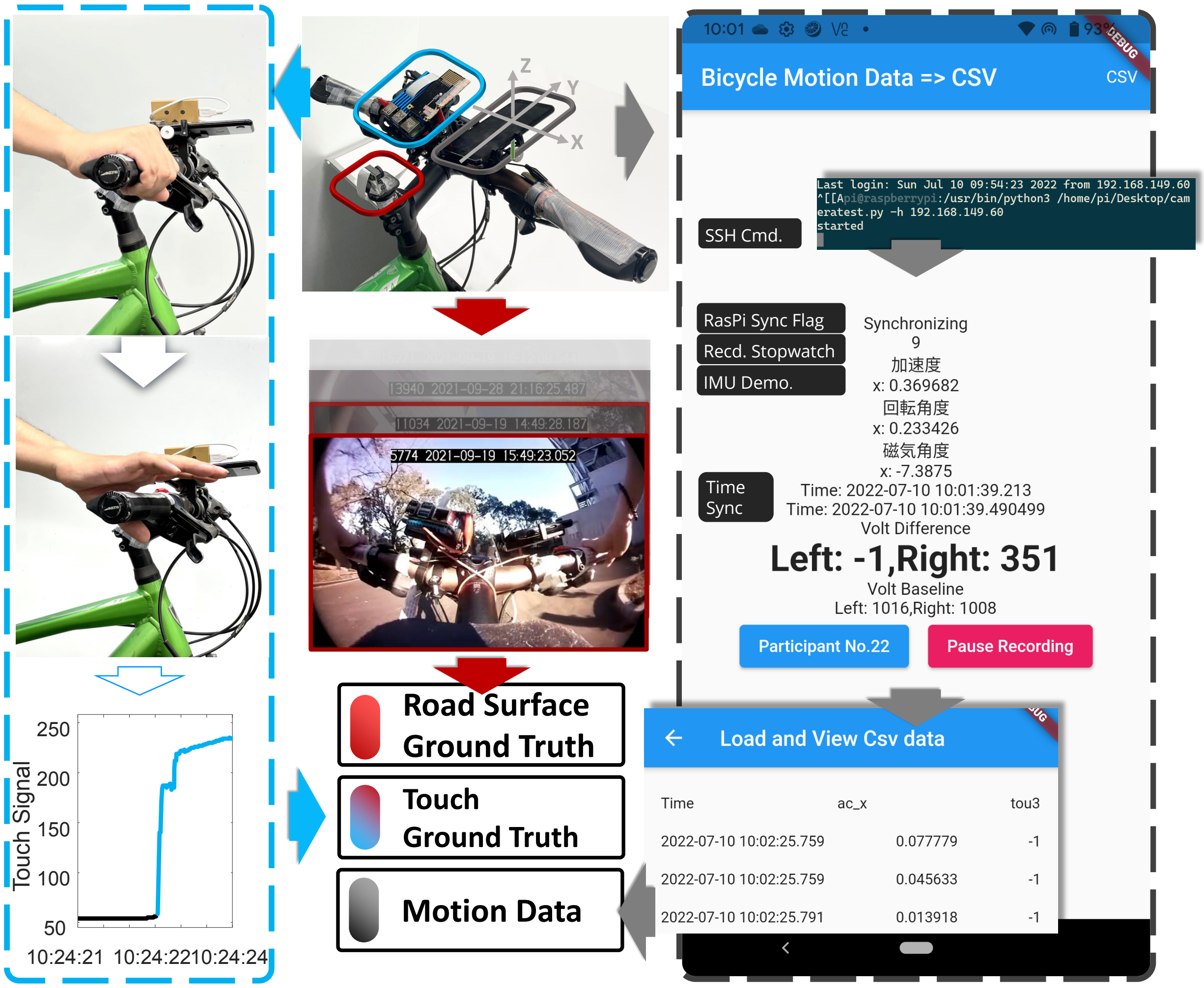

Figure 3.3 Data collection platform, including hardware, dataflow and user interface.

classification accuracy with lower time solution. We further investigates the impact of sliding window length in Sec. 4.2

3.2.3 Feature Extraction

Next, we applied the VAR model and wavelet scattering network models to yield representative subtle features from the motion reading. Previous studies have employed similar techniques in electrocardiogram-derived cycle heartbeat recognition applications [39, 40]. Similarly, periodic circular movement components can be derived when monitoring bicyclist data. We Regarding the time-frequency domain analysis, the short-time Fourier transform (STFT) and wavelet transform (WT) were compared for use in our time-frequency analysis. Notably, the STFT is less sensitive to abrupt frequency fluctuations that occur when cyclists change positions, such as removing a

Table 3.1 Feature selected.

Model	Features
VAR	Coefficients of Lag-4 $\{A_i\}$
Wavelet	Min, max, average skewness of each path, varience of all

hand during cycling. It is also more computationally intensive than WT, resulting in faster battery consumption and higher response latency when deployed on mobile platforms. Therefore, the WT-based method was chosen.

Vector Autoregressive Model

The VAR model is a classical stochastic process method used for time-series analysis. Accordingly, in a stationary time series of a variable vector $\{w_t\}$, the value of step s, w_s, is linearly related to the values of all elements in latest p steps before step s:

$$w_s = \sum_{i=1}^{p} A_i w_{s-i} + \epsilon_s$$

The formula represents a Lag-p VAR model with a coefficient matrix set, $\{A_i\}, (i \leq p)$, where A_i stands for a constant n-by-n matrix for the latest i step values. n is the length of vector w_s. Note that $\{\epsilon_s\}$ is a zero-mean white-noise term. After attempts with multiple p, we found that two order-3 & Lag-4 models of separated accelerometer and gyroscope input achieved the best result; hence, we configured our method with such settings. A maximum likelihood-based approach is adopted to estimate model coefficients[41]. Noted that through the pilot study in Section 3.1.2 we found the acceleration date fits the stationary criteria, while the angular speed data can only fit it after being differentiated. Therefore we take the accelerometer data and the differential of gyroscope data as input for VAR model. This does not apply to the wavelet scattering network.

Wavelet Scattering Network

A wavelet network was proposed [42] to carry out a wavelet time scattering decomposition so that steady features from time sequences can be analyzed while maintaining category divergence. It consists of a repeated process using three operators (i.e., wavelet transform, modulus, and averaging) in every node of a tree structure. There are some similarities between wavelet scattering networks and deep neural networks. However, the coefficients of the former are predefined in filters rather than trained. For HAND DETECTION, we applied an order-one network with a filter bank containing three wavelets per octave. From each time window, a scattering coefficient matrix was

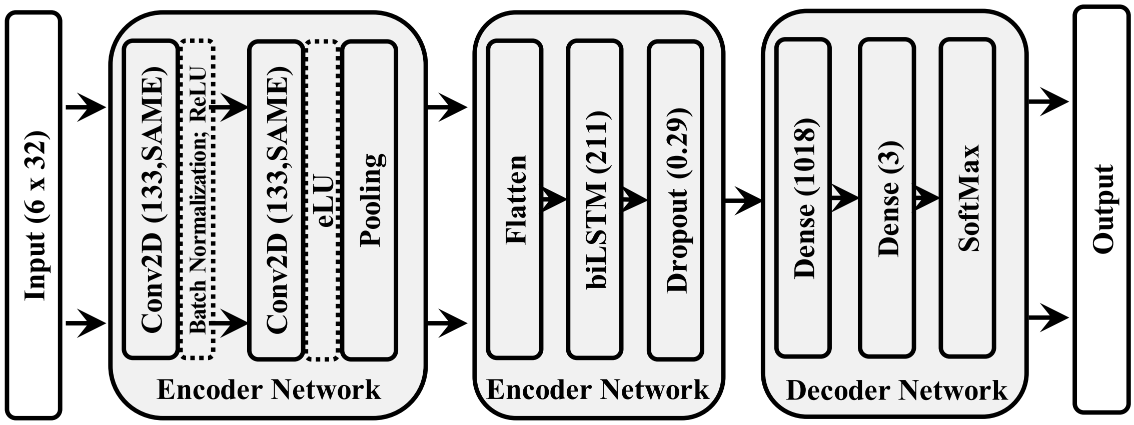

Figure 3.4 DoubleCheck's neural network layout.

produced with a size of 5×10, representing five scattering paths in each of the 10 temporal slots. For DISTRACTION RECOGNITION, the filter bank was expanded to eight wavelets per octave, and the coefficient matrix size was increased to 13×8. A more complicated network is possible with prolonged window lengths. However, for this experiment, we employed only the Gabor wavelet in the filters.

Overall, we adopted 144 features for every hand-detection time window and 192 for distraction-recognition ones. Table 3.1 lists the features extracted for each axis of acceleration and angular speed.

3.2.4 Detection

We chose an SVM with a cubic polynomial kernel to classify the three cycling handgrip situations (i.e., left, right, and two). The SVM classifier is lightweight enough to be battery-friendly, and it categorizes scattering and AR coefficients effectively [40, 42].

Once single-handed cycling is detected, a lightweight neural network classifier would be leveraged to identify the distraction cycling activities of Take-from-Pocket and Phone-Tab. The combined CNN-RNN network is demonstrated to be effective in the processing of time-frequency features of IMU signal [43]. Fig. 3.4 presents the architecture of DoubleCheck's BiLSTM-based neural network design. Our network possesses only 4 layers to meet the requirement of the mobile platform. We input the data in forms of $6 \times (12 + 28)$ $(Num\_axes \times (Num\_AR\_features\_per\_axis + Num\_wavelet\_features\_per\_axis))$.

Chapter 4

Evaluation of DoubleCheck in Campus Study and Limited Urban Road Study

As claimed in Section 3.1, we endeavor to detect single-handed cycling behaviors in a real-time manner by DoubleCheck. Thus there comes the question regarding the usability and robustness of our method:

How efficient is DoubleCheck in **Q1:** detecting single-handed cycling behavior, **Q2:** extended scope in determining the exact cycling hand(s), and recognizing distraction cycling behaviors?

We respond to the above questions with evaluation of HAND DETECTION and DISTRACTION RECOGNITION.

4.1 Experiment Protocol

Comprehensive experiments have taken more than 2 months to construct the dataset. Our cycling experiment is permitted by the Institutional Review Board (IRB) of the Center for Spatial Information Science, the University of Tokyo.

Campus study

We invited 22 participants (13 males and 9 females) to join our experiment. All of them possess single-handed cycling skills. Before formal data collection, the participants were briefed on the task, route, and cycling safeguards. All of them were allowed a few minutes of test rides. The safety measures taken included the provision of helmets and protections for elbows, hands, and knees. We also adjusted the saddle height of the test bike for every rider according to their stature.

(a) Routes for Campus Study.

(b) Route for Limited Field Study.

Figure 4.1 Experiment routes and road surfaces for Hand Detection (Left, Both, Right-handed Cycling) and Distraction Recognition (Take-from-Pocket, Smartphone Tap). For every route, the participant is asked to ride equal times in two directions.

The controlled experiment route was only within our university campus, composed of an asphalt section and a pavement section (Fig. 4.1a). The flagstone-paved pavement path is somewhat rugged and risky so the arrangement contains only a straight path while for the asphalt road, there are eight left turns and another eight right turns. Both contain manholes.

Overall, each of the participants performs several cycling behaviors on our test bike:

Hand Detection: *Left-hand cycling on road (Left-R), left-hand cycling on pavement (Left-P), normal cycling on road (Both-R), normal cycling on pavement (Both-P), right-hand cycling on road (Right-R), right-hand cycling on pavement (Right-P).* Noted that during single-handed cycling, the rider is asked to drop the spare arm naturally beside his or her body unless otherwise explained.

Distraction Recognition: *Taking from Pocket (Take-from-Pocket), Smartphone Tap (Phone-Tap).* Our recording smartphone stays mounted on the handlebar. All distraction cycling is carried out on the asphalt road as a proof-of-concept experiment.

A whole process takes one person about an hour with three to four minutes of cycling for each cycling behavior. Intervals for rest take two to five minutes or more time if the cyclist is tired. In total, we have sorted and labeled cycling data for about 6.5 hours long. The ratio of asphalt road and pavement sections are roughly equal. The recording application is later found to have crashed several times during cycling behaviors that involved smartphone usage. Consequently, we successfully collected all 22 persons' data for HAND DETECTION and 14's for DISTRACTION RECOGNITION.

The data is labeled by signals from the tactile sensor (Fig. 3.3). We manually proofread all the labels with the cycling log video. Our tactile sensor works for the better part of experiments. The latency of hand switching between the touch signal and video frame is within 80 milliseconds with proper configuration.

Limited Urban Road Study

After fine-graining parameters and collecting training data, we materialized the trained model as a smartphone application. Another 5 participants (3 Males and 2 Females) are invited to evaluate the integrated application. However, participants were only asked to implement *normal cycling on road* in real city roads outside the campus due to safety concerns.

4.1.1 Metrics in Evaluation

The assessment of our model in the following part is through 10-fold cross-validation (10-Fold) and leave-one-member-out cross-validation (LOMO). The former helps to enable a benchmark future works around single-handed cycling issues. While the latter evaluates the model's inter-user

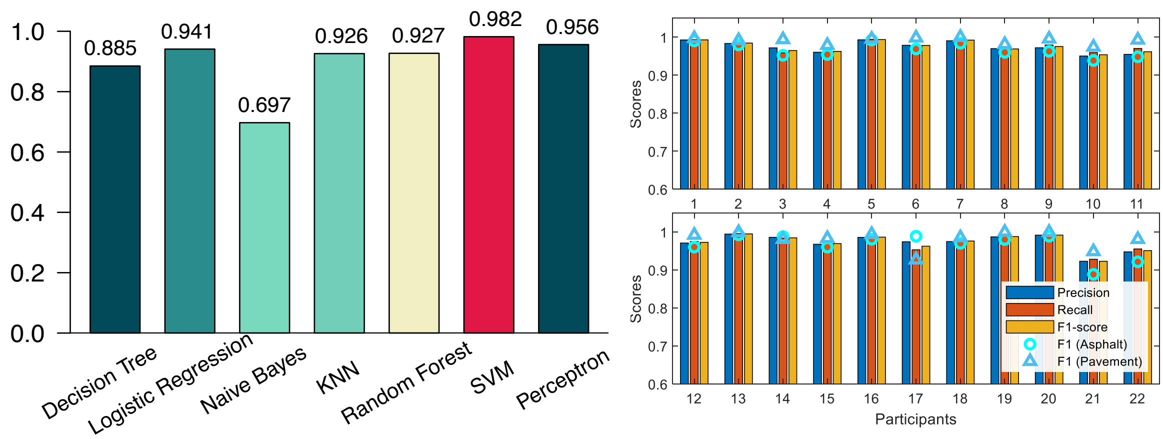

(a) Comparison with other classifiers (10-Fold). (b) Per subject performance (LOMO).

Figure 4.2 Outcome of Hand Detection (Single vs. Both).

generalizability, which in this context strongly relates to the real-world performance since DoubleCheck can require no amount of single-handed cycling data from a new user for personalization. The assessment metric computed in the cross-validation includes *recall*, *precision*,*F1-score*, and *false position rate (FPR)*. A model with higher recall in prediction would overlook fewer single-handed cycling events, whereas one with high precision would make detection where most of the detected single-handed events were actually happening at that time. The F1-score averages the value of recall and precision. Additionally, low FPR stands for nearly no false alarm being made from normal double-handed cycling.

4.2 Q1: Hand Detection: Single vs. Both

4.2.1 Overall Performance of Campus Study

We first explore the accuracy of our method's core objective: binary classification. We leverage 10-Fold to evaluate the SVM in comparison with other recurring methods in human activity recognition researches: Decision Tree, Logistic Regression, Naive Bayesian, kNN, Random Forest, and Perceptron. The result in Fig.4.2a displays two massages: 1) the SVM outperforms the else approaches with higher F1-score and should be adopted in HAND DETECTION; 2) methods like Perceptron also reach high accuracy, further proving our extracted features are effective. For LOMO, the F1-score of DoubleCheck also exceeds 0.97. Fig. 4.2b displays the detailed performance. The worst case happens with the 21st participant whose F1-score is 0.92, proving our system to be an effective check against single-handed cycling across the individual variety, satisfying the intrinsic requirement of user independence in practical dangerous cycling detection.

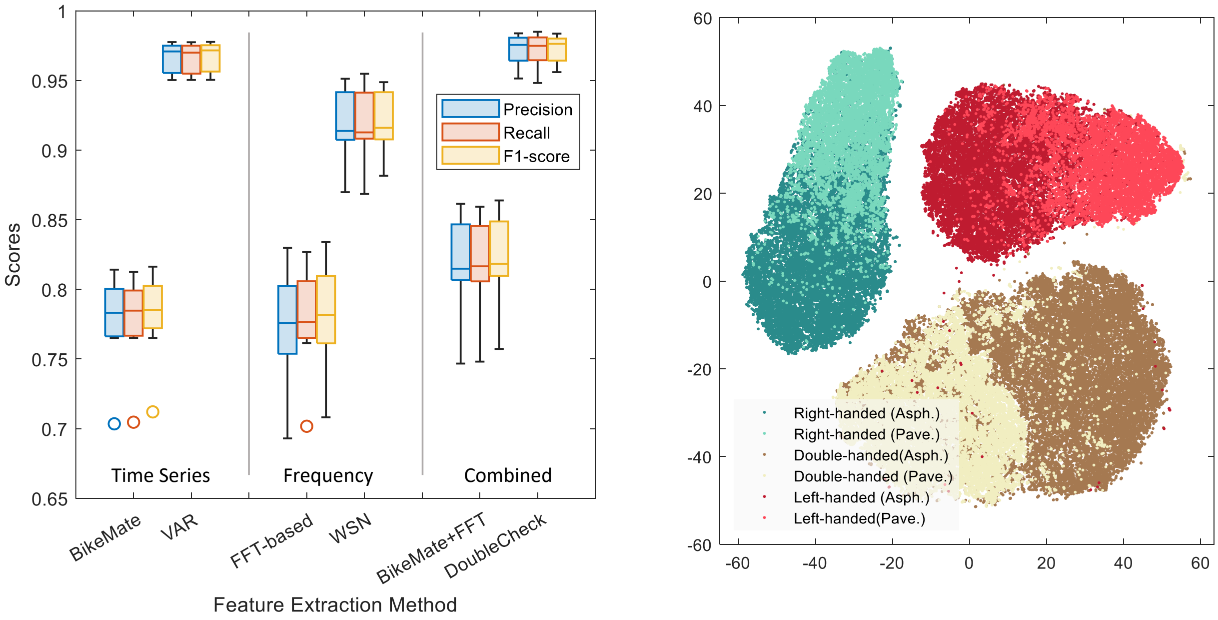

(a) Comparison of feature extraction method (LOMO). (b) Visualization of extracted features with t-SNE.

Figure 4.3 Performance of feature extraction method of DoubleCheck.

4.2.2 Credits of VAR and Wavelet Scattering Network (WSN)

In this section, we evaluate how DoubleCheck benefits from the VAR and WSN models. As the account in Sec. 3.2.3, we utilize the vector autoregressive model and wavelet scattering network to retrieve temporal and frequency features related to movement pattern changes brought by single-handed cycling. We draw the t-Distributed Stochastic Neighbor Embedding (tSNE) of the extracted features of All participant's data in Fig. 4.3b. The figure indicated most of the motion data of double-handed cycling and single-handed cycling have been clearly separated by our method. Furthermore, to validate the effectiveness of these two approaches, we implemented two other baseline feature extraction methods in respective to the temporal and frequency domain:

- BikeMate: BikeMate[24] is the most similar related system also targeting dangerous cycling behavior. Its feature extraction method for IMU signal computes a vector of five features for each axis of accelerometer and gyroscope: *sum*, *standard deviation*, *average absolute difference*, *binned distribution*, and *distance for the greatest correlation coefficient*.
- Fast Fourier Transform-Based: We derived the power spectrum of the sliding window data through FFT and calculated same features for WSN listed in Table 3.1.

We trained SVM models mentioned in Sec. 3.2.4 by derived features from single and both methods. The models were evaluated models with LOMO. Fig. 4.3a presents the differences in performance. For these two sets of temporal-frequency methods, the concatenation of features has generally boosted accuracy. The combined features of BikeMate and the FFT-based land both the average precision and recall more than 0.82, which is more than 10% below the result of either WSN or VAR and thus clearly outperformed. Tabel 4.1 displays more detailed results with varying window lengths. We can tell that the VAR model is more competitive in terms of the average F1-score of 0.93 with only data of 0.3-second length (24 samples). However, the F1-score collapsed and FPR exploded suddenly when the window length is reduced to 0.1 second. While the WSN helps the combined model maintain a practical F1-score of 0.85.

4.2.3 Credits of Accelerometer and Gyroscope

To apprehend how each sensor contributes to the detection of single-handed cycling, we broke down the Campus Study data by source sensor and trained models with separated data. In general, data of angular speed from gyroscope could singly achieve a satisfying F1-score above 0.90 with the sampling rate in the sampling rate of 32Hz. Table. 4.2 shows the result of the ablation study for each sensor. We observed that gyroscope-only input in 32Hz could achieve an F1-Score more than 0.9 and an FPR under 0.1 in single-handed cycling detection. Acceleration data is not as competitive but also enables detection with F1-scores and FPR in this standard in a 60Hz sampling rate. The combination of both sensors would bring steady growth in F1-score and more significantly, a suppression in FPR, demonstrating each sensor is useful. We can conclude that DoubleCheck is compatible with cheap devices with only the accelerometer. However, devices with 6-axis IMU could enjoy better performance.

4.2.4 Impact of Sliding Window Size

Given the excellent performance under the designated configuration in Sec. 3.2, a question could naturally come to viewers what would be the least amount of data DoubleCheck needs to achieve various levels of performance. Usually, a shorter window means higher temporal resolution at the cost of decreased accuracy. Therefore, a balanced choice is needed. We applied a range of window sizes with 0.5 overlap rate to the Campus Study data sampled at 80Hz and trained and assess the model in the LOMO way. The method performance with varying sliding window sizes is shown in Table. 4.1. Overall, our method exhibits robustness with a decreased amount of input. The hand detection holds an F1-score over 0.91 with windows longer than 0.2 second (16 points

Table 4.1 Performance of hand detection under different window sizes (LOMO).

	VAR Only(%)		WSN Only(%)		Combined(%)	
Sliding Win.	*F1-Score*	*FPR*	*F1-Score*	*FPR*	*F1-Score*	*FPR*
0.1s	38.35	525.67	82.38	21.43	85.39	18.29
0.2s	88.61	14.37	85.64	18.46	91.64	10.33
0.3s	92.85	08.36	88.35	14.84	94.45	6.72
0.4s	95.53	5.22	89.83	13.05	96.37	4.37
0.5s	96.71	3.82	92.05	9.98	97.30	3.25
0.6s	97.70	2.70	95.23	6.24	98.25	2.31
1.0s	98.37	1.89	96.59	4.73	98.78	1.63

Table 4.2 Performance of hand detection under different sampling frequencies (LOMO).

	Acc. Only(%)		Gyro. Only(%)		Six-Axis(%)	
Samp. Rate	*F1-Score*	*FPR*	*F1-Score*	*FPR*	*F1-Score*	*FPR*
16Hz	72.34	37.31	80.97	23.64	83.20	21.40
20Hz	76.03	33.22	86.47	16.66	88.49	14.32
32Hz	81.21	24.43	91.79	9.90	93.09	8.38
40Hz	82.44	23.10	91.98	9.72	93.47	8.05
50Hz	87.90	14.90	93.45	7.75	95.45	5.66
60Hz	91.67	9.86	94.86	6.14	96.88	3.89
80Hz	92.95	8.35	95.17	5.67	97.28	3.27

of samples). On the other hand, there is FPR and F1-score improvement in small steps along the window length growth from 0.2s till the investigated range, and the best performance is reached with 0.99 and 0.02 under the window length of 1.0 second. We considered a window length of 0.5s as accurate enough in both time resolution and detection rate and adopted it in our method.

4.2.5 Impact of Sampling Rate

In this section we look into the influence of different sampling rates on the performance of hand detection. A lower sampling rate stands for less power consumption and usually performance compromise. We trained models upon FIR filter-resampled data from the Campus Study with 0.5-second window. Table 4.2 presents the hand detection performance of DoubleCheck under

Table 4.3 Performance of hand detection under Limited Urban Road Study.

Experiment subject	Sub 1	Sub 2	Sub 3	Sub 4	Sub 5
FPR(%)	4.82	3.60	2.11	4.36	13.76

various sampling frequencies from 16 to 80Hz. The results indicate that our method can indeed identify single-handed cycling with a promising F1-score of 0.88 and an FPR of 0.14 even with a low 20Hz sampling frequency, enabling the implementation in some battery-restrained embedded platforms. We considered an F1-score of 0.95 and FPR 0.6 as accurate enough to alleviate the risk of overfitting, especially for the controlled simulation experiment. Therefore we chose 50Hz as the sampling rate in the prototype integration of DoubleCheck later used in the Limited Urban Road Study.

4.2.6 Impact of Road Surface

Fig. 4.2b shows the capability comparison of DoubleCheck on asphalt and pavement (4.1a). For all participants except one, the method yields better results on the pavement. The outcome accords with our analysis in Section 3.1.2that rugged road surfaces tend to amplify single-handed cycling-brought differences in movement features. However, the classifier still attains high accuracy on asphalt road with an average F1-score of 0.97. The curve displays the robustness of our method to different road surfaces.

4.2.7 Performance of Limited Urban Road Study

The above analysis of Campus Study has validated the performance of DoubleCheck in the detection of single-handed cycling under simulated conditions. To answer the question about the ecology validity, we next peek into the robustness of our method under real-world traffic scenarios by analyzing the data from the Limited Urban Road Study. Note that we could only calculate the FPR due to the constrained data collection with only double-handed cycling. Table. 4.3 displays the per-participant performance. The average FPR is 0.06. Though it seems close to that of the Campus Study result in Table 4.2, the error rate of fake alarms exploded in Subject 5. One reason to attribute this is that after checking the video, we found Subject 5 experienced a short range of traffic jams, while the other subjects were cycling with relatively smoother traffic. This motivates us to conduct more real road studies with less controlled conditions to assess and improve the actual performance in the future.

Table 4.4 Precision, recall, F1-score, and false positive rate of exact cycling hand(s) detection (Left vs. Right vs. Both).

	Left		Both		Right	
Metrics	*10-Fold*	*LOMO*	*10-Fold*	*LOMO*	*10-Fold*	*LOMO*
Precision(%)	93.19	90.01	95.56	93.85	94.51	92.58
Recall(%)	92.91	90.35	95.4	93.06	95.07	93.58
F1-score(%)	93.05	90.22	95.48	93.45	94.79	93.08
FPR(%)	2.72	3.7	3.76	4.99	1.86	2.42

4.3 Q2: Extended Scope

Having reached satisfying precision in the binary case, we seek to make a more detailed explanation of cycling hand detection with our method for extracting its potential for extended applications proposed in Sec. 5.1.1.

4.3.1 Hand Detection: Left vs. Right vs. Both

We re-labeled the data with the exact hand used in cycling and ran the LOMO validation. The results are shown in Table 4.4, from which we can observe that DoubleCheck is fully capable to determine the exact hand(s) used in cycling with values of precision and recall exceeding 0.94 at 10-Fold and 0.92 at LOMO. Moreover, the false positive rates (FPR) in both cases are kept below 0.05.

Next we analyze how the user diversity would influence the performance of the HAND DETECTION. Since the accuracy of triple classification is overall high, we carry out a six-class classification (Left vs. Right vs. Both, Road vs. Pavement) to better expose the user dimension differences. The F1-scores are 0.89 (10-Fold) and 0.84 (LOMO). We conduct a survey within our participants after the experiment, about their cycling proficiency based on five categories (*Novice, Intermediate, Strong Intermediate, Proficient, Very Proficient*). The whole personnel possesses no less than the second level (0:1:8:7:6). As presented in Fig. 4.4a, If we quantify the categories from 1 to 5, an observation can be drawn that the closer a user's proficiency is to the average level—around category *Proficient* in this case—the better his or her classification result in LOMO tends to be. This accords with the mechanism of LOMO.

We have 13 male and 9 female cyclists in the Campus Study and the average result of the two

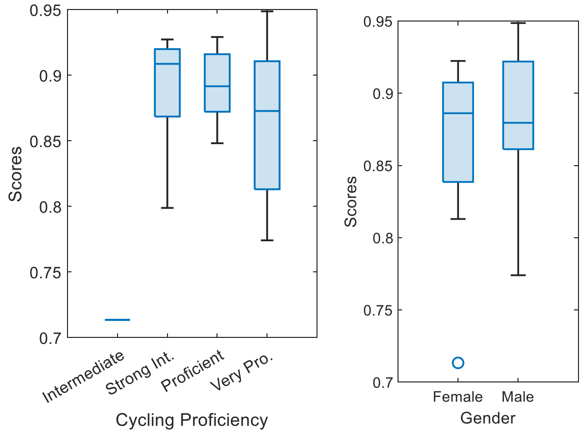

(a) (b)

Figure 4.4 User study of Hand Detection (Left vs. Right vs. Both, Road vs. Pavement).

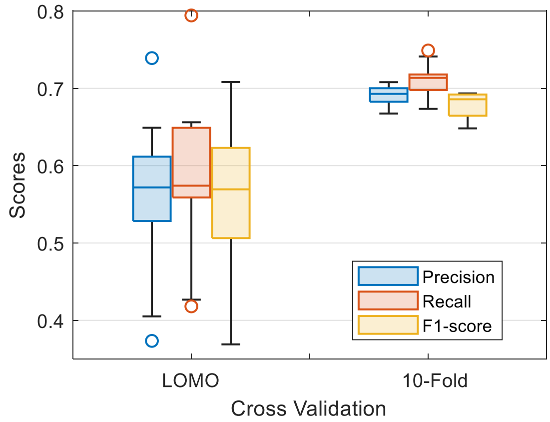

Figure 4.5 Performance of Distraction Recognition Under D.

genders is plotted in Fig. 4.4b, where we could see the system accuracy is nearly the same for males and females. The male scores are slightly higher in the median. One possible explanation is the gender imbalance in training sets has resulted in the bias of our model.

4.3.2 Distraction Recognition Result

Given the high accuracy in hand detection, particularly the binary classification, we evaluate the distraction recognition given the single-handed cycling scenario. For the training dataset, a proper portion of samples from classes *Left&Right-R* composes the class *Hand-Drop*. Recognition performance is presented in Fig. 4.5 The average F1-score in 10-Fold is 0.69. The numbers drop to 0.57 in LOMO. The results imply that the distraction behaviors within our scope can somehow affect motion patterns, yet the differences may be very blurred and unstable regarding our current recognition scheme. We need to further improve our understanding of the behavior features. The greatest confusion is between class *Take-from-Pocket* and *Hand-Drop*. One explanation is that the former contains the process of fetching and returning stuff, during which the rider's eyes are not necessarily taken off from the road. Consequently, their balance tends to be as less affected as *Hand-drop*.

Chapter 5

Discussion and Conclusion

5.1 Discussion and Future Works

Having evaluated the performance of our system, we would further discuss interpretations, limitations, and future improvements in this section.

5.1.1 Opportunities for DoubleCheck

Bike Integration

Our method provides a detection service from a handlebar-borne IMU using a smartphone and an RPi for processing. We predict that IMU capabilities will be sufficiently adapted to smartphones soon, which will further minimize the hardware burden. This would be particularly useful for bike-sharing services, as long as the bikes are instrumented with IoT devices such as the processing and communication units in advance. Detected hazardous single-handed cycling behaviors could also be used to trigger acoustic alerts to nearby vehicles with the proper speaker equipment. The collected data could also assist forensic and accountability efforts for bike-involved accidents.

Turning Light Switch

The use of bike-mounted turning lights also qualifies as a single-handed event. Hence, it would be useful to use DoubleCheck in place of physical switches, considering the tool’s precise riding hand identification (e.g., hand signaling). Doing so would require new hardware, but it would reduce distraction even further.

Upper-Limb Muscle Tension as Input

DoubleCheck demonstrated that changes in control ability based on upper-limb activity are distinguishable when using an IMU and our machine-learning approach. The possibility of integrating hand-grip and muscle tension measures should also be explored, as it may serve as a convenient interaction method that does not require single-handed cycling.

5.1.2 Limitations

This is one of several gap-filling advancements toward achieving the challenging mission of ubiquitous cycling safety monitoring and alerting. Notably, DoubleCheck has several limitations that future works should remedy.

The main shortcoming of this research is the shortage of field studies. Realistic cycling environments and diverse behaviors create far more complexity than was accounted for in our controlled environment. For example, bicycle types, velocities, gear ratios, slopes, and off-road terrains were not considered. They will certainly have a strong influence on cycling movement patterns. DoubleCheck should be made more robust to such variables. Moreover, we noticed that it is more difficult to successfully categorize the road conditions of subjects who routinely ride fast. Furthermore, our participant count was too small to offer comprehensive generalizations. For these reasons, future studies should be conducted on a larger scale and in open environments.

The limited scope of this study could also be identified as a drawback. Furthermore, the accuracy of classifying the distraction activities of the spare hand should be improved. Additional behaviors, such as holding an umbrella, making a hand-held phone call, reaching for bottles, and drinking are no less pervasive than the ones analyzed in our study (Fig. 1.1). However, such single-handed activities may employ motions too far away from the handlebars, making hazard prediction less accurate and testing more dangerous. Future work should employ simulated kinetic data for these reasons. Various motion pattern discrepancies should also be investigated for improved accuracy. Additional platforms, such as modern wrist-worn sensing devices, are strong candidates for accurately detecting hand actions [19].

To the best of our knowledge, DoubleCheck is merely available for detecting ongoing danger. The production and analysis of steering logs would provide an improved approach to reinforcing cyclist vigilance, as trips could be reviewed, and mistakes could be quantified. To achieve this, a logic filter is needed to rule-out spurious data from cycling anomalies. Furthermore, by using GPS tracking data alongside those already captured, it may be possible to predict the probability of single-handed cycling based on location.

5.2 Conclusion

In this paper, we proposed DoubleCheck: a smartphone-based cycling aid focusing on single-handed cycling and enabling hand detection and distraction recognition. We leveraged an embedded tri-axial accelerometer and gyroscope to acquire motion readings and introduced an AR model with a wavelet scattering network, which yielded representative cycling activity. Experiments with 22 subjects demonstrated the performance of our system with an F1-score of 0.97 for the accurate detection of cycling hand(s) and with a score of 0.69 for accurately identifying distracted cycling behaviors. We further investigated the influence of user diversity on system performance and provided future opportunities for DoubleCheck. We envision that our work will facilitate safer bicycle commuting with no more than a software update on a smartphone, and it will shed light on future schemes for mobile riding interactions.

Publication

[1] Dong, X., Han, Z., Nishiyama, Y., & Sezaki, K. (2022, October). DoubleCheck: Single-Handed Cycling Detection with a Smartphone. In 2022 IEEE International Conference on Systems, Man, and Cybernetics (SMC) (Accepted). IEEE.

[2] Han, Z., Dong, X., Nishiyama, Y., & Sezaki, K. (2022, June). Head dynamics enabled riding maneuver prediction. In Proceedings of the 20th Annual International Conference on Mobile Systems, Applications and Services (MobiSys'22) (pp. 557-558).

[3] Dong, X., Han, Z., Nishiyama, Y., & Sezaki, K. (2022, March). DoubleCheck: Detecting Single-Hand Cycling with Inertial Measurement Unit of Smartphone. In 2022 IEEE International Conference on Pervasive Computing and Communications Workshops and other Affiliated Events (PerCom Workshops) (pp. 50-53). IEEE.

[4] Dong, X., Han, Z., Nishiyama, Y., & Sezaki, K. (2021, September). Detecting Single-Hand Riding with Integrated Accelerometer and Gyroscope of Smartphone. In Adjunct Proceedings of the 2021 ACM International Joint Conference on Pervasive and Ubiquitous Computing (UbiComp'21) (pp. 19-20).

[5] Han, Z., Dong, X., Nishiyama, Y., & Sezaki, K. (2021, September). HeadSense: A Head Movement Detecting System for Micro-Mobility Riders. In Adjunct Proceedings of the 2021 ACM International Joint Conference on Pervasive and Ubiquitous Computing (UbiComp'21) (pp. 26-27).

Acknowledge

Should you skip the content, I strongly recommend you to read it first, since I define it as interesting.

The world has kept being, quoted from the acknowledgment of my undergraduate thesis two years ago, so unexpected. Consequently, the support and love I received is more valuable on rainy days. Many thanks to a bunch of people need to be delivered here.

I would like to thank Prof. Kaoru Sezaki for the given opportunity and supervision during these two years. The given advice and patience are invaluable.

In addition, I want to extend my thanks to Prof. Nishiyama Yuuki, for his insightful comments and onsite help for my research every day in the laboratory. Being the Iron Man of the laboratory, he has been inspiring me and other members of Sezaki Lab with his always passionate mentality.

I would like to thank the co-advisor, Prof. Song Xuan for his constructive guidance and review.

Also, sincere gratitude needs to be expressed to my fellow laboratory members: future Dr. Zengyi Han, future Dr. Hidenaga Ushijima, future Dr. Liqiang Xu, and future Dr. Hidenaga Ushijima, future Dr. Helinyi Peng, future Dr. Eri Hosonuma. future Dr. Shoto Ono, future Dr. Suxing Lyu Mr. Duc Nguyen, Ms. Chen Meiyi, Mr. Yutaro Koike, Ms. Tiantian Jiang, Ms. Soichiro Higuma, Mr. Ruichao Zhang, Mr. Riku Ishioka, Mr. Ao Tang, Mr. Ryoto Suzuki, Mr. Yuki Kasahara, Mr. Kazuki Shimojo, Mr. Haoyu Zhuang. Han has taught me a lot in research, from nuts and bolts to other esoteric words. The hiking with Duc, Ushijima, Chen, and Tang is always interesting. Many of you have witnessed and experienced life before Covid-19 at the University of Tokyo, and thus got nostalgia from time to time. However, I already define my laboratory life with you as brilliant. Furthermore, I need to thank three secretaries of Sezaki Lab for their hard and professional work: Ms. Kaho Matsumoto, Ms. June Naito, and Ms. Yuka Yoneda.

There are sincere feelings about other friends. future Dr. Yichen Song has passed precious experience in human activity recognition-related time series analysis. The constructive suggestion about signal processing from future Dr. Menghan Lin is quite helpful. I am also grateful to future

Dr. Mingxin Zhang for my consult about deep learning. Thank you my friends from the Chinese Basketball Club of the University of Tokyo, let's keep playing and keep making progress.

My whole family, including but not restricted to my mother, father, paternal grandfather, paternal grandmother, maternal grandmother, and maternal grandfather need to be specially thanked for the love and strong support, without which I would have no chance of completing this study.

There must be other people I would have thanked yet failed to do so. I wish you all the way I wish myself to be: find what your love and the opportunity to practice. Hope I could speak without hesitation that I have a Master's diploma from the University of Tokyo.

References

[1] W. H. Organization, "Global status report on road safety 2018," World Health Organization, 2018. [Online]. Available: https://www.who.int/publications/i/item/9789241565684/

[2] E. S. Wolfe, S. S. Arabian, J. L. Breeze, and M. J. Salzler, "Distracted biking: An observational study," *Journal of Trauma Nursing*, vol. 23, p. 65–70, 2016.

[3] M. de Angelis, F. Fraboni, V. M. Puchades, G. Prati, and L. Pietrantoni, "Use of smartphone and crash risk among cyclists," *Journal of Transportation Safety & Security*, vol. 12, pp. 178 – 193, 2019.

[4] D. De Waard, B. Lewis-Evans, B. Jelijs, O. Tucha, and K. Brookhuis, "The effects of operating a touch screen smartphone and other common activities performed while bicycling on cycling behaviour," *Transportation Research Part F: Traffic Psychology and Behaviour*, vol. 22, pp. 196–206, 2014. [Online]. Available: https://www.sciencedirect.com/science/article/pii/S1369847813001320

[5] N. P. Agency, "Annual report of traffic accident statistics of 2020," 2021. [Online]. Available: https://www.npa.go.jp/publications/statistics/koutsuu/toukeihyo_e.html

[6] R. K. Brandt, S. Haustein, and M. Møller, "Cyclists' phone use in relation to proximate environmental characteristics - a qualitative study," *Journal of Transport & Health*, vol. 23, p. 101283, 2021. [Online]. Available: https://www.sciencedirect.com/science/article/pii/S2214140521003133

[7] X. Fan, F. Wang, D. Song, Y. Lu, and J. Liu, "Gazmon: Eye gazing enabled driving behavior monitoring and prediction," *IEEE Transactions on Mobile Computing*, vol. 20, no. 4, pp. 1420–1433, 2019.

[8] J. Xie, A. R. Hilal, and D. Kulic, "Driver distraction recognition based on smartphone sensor data," in *2018 IEEE International Conference on Systems, Man, and Cybernetics (SMC)*, 2018, pp. 801–806.

[9] T. Kamimura, T. Kitani, and T. Watanabe, "A system to comprehend a motorcycle's behavior using the acceleration and gyro sensors on a smartphone," *Global Research and Education*,

vol. 8, 2012.

[10] A. Costes, N. A. Turpin, D. Villeger, P. Moretto, and B. Watier, "Influence of position and power output on upper limb kinetics in cycling." *Journal of applied biomechanics*, vol. 32 2, pp. 140–9, 2016.

[11] X. Dong, Z. Han, Y. Nishiyama, and K. Sezaki, "Detecting single-hand riding with integrated accelerometer and gyroscope of smartphone," in *Adjunct Proceedings of the 2021 ACM International Joint Conference on Pervasive and Ubiquitous Computing and Proceedings of the 2021 ACM International Symposium on Wearable Computers*, ser. UbiComp '21. New York, NY, USA: Association for Computing Machinery, 2021, p. 19–20. [Online]. Available: https://doi.org/10.1145/3460418.3479294

[12] S. Wang, C. Chen, and J. Ma, "Accelerometer based transportation mode recognition on mobile phones," in *2010 Asia-Pacific Conference on Wearable Computing Systems*. IEEE, 2010, pp. 44–46.

[13] S. B. Eisenman, E. Miluzzo, N. D. Lane, R. A. Peterson, G.-S. Ahn, and A. T. Campbell, "Bikenet: A mobile sensing system for cyclist experience mapping," *ACM Transactions on Sensor Networks (TOSN)*, vol. 6, no. 1, pp. 1–39, 2010. [Online]. Available: https://doi.org/10.1145/1653760.1653766

[14] D. Krumm and S. Odenwald, "Development of a dynamometer to measure grip forces at a bicycle handlebar," *Procedia Engineering*, vol. 72, pp. 80–85, 2014, the Engineering of Sport 10. [Online]. Available: https://www.sciencedirect.com/science/article/pii/S1877705814005335

[15] A. Trujillo-León, W. Bachta, J. Castellanos-Ramos, and F. Vidal-Verdú, "Assistive handlebar based on tactile sensors: control inputs and human factors," *Sensors*, vol. 18, no. 8, p. 2471, 2018.

[16] J. Vanwalleghem, I. De Baere, M. Loccufier, and W. Van Paepegem, "Dynamic calibration of a strain gauge based handlebar force sensor for cycling purposes," *Procedia Engineering*, vol. 112, pp. 219–224, 2015.

[17] A. Dancu, V. Vechev, A. A. Ünlüer, S. Nilson, O. Nygren, S. Eliasson, J.-E. Barjonet, J. Marshall, and M. Fjeld, "Gesture bike: Examining projection surfaces and turn signal systems for urban cycling," in *Proceedings of the 2015 International Conference on Interactive Tabletops & Surfaces*, ser. ITS '15. New York, NY, USA: Association for Computing Machinery, 2015, p. 151–159. [Online]. Available: https://doi.org/10.1145/2817721.2817748

[18] M. Bonilla, P. Córdova, D. Jiménez, and A. Robayo, "Monitoring system of physiological signals with emergencies management for the road safety of cyclists," in *2019 Sixth Interna-*

tional Conference on eDemocracy & eGovernment (ICEDEG), 2019, pp. 274–279.

[19] C. Bi, J. Huang, G. Xing, L. Jiang, X. Liu, and M. Chen, “Safewatch: A wearable hand motion tracking system for improving driving safety,” vol. 4, no. 1. ACM New York, NY, USA, 2019, pp. 1–21.

[20] G. Rybarczyk, A. Ozbil, E. Andresen, and Z. Hayes, “Physiological responses to urban design during bicycling: A naturalistic investigation,” *Transportation Research Part F: Traffic Psychology and Behaviour*, vol. 68, pp. 79–93, 2020. [Online]. Available: https://www.sciencedirect.com/science/article/pii/S1369847819304474

[21] S. Miah, E. Milonidis, I. Kaparias, and N. Karcanias, “An innovative multi-sensor fusion algorithm to enhance positioning accuracy of an instrumented bicycle,” *IEEE Transactions on Intelligent Transportation Systems*, vol. 21, no. 3, pp. 1145–1153, 2020.

[22] N. Thepvilojanapong, K. Sugo, Y. Namiki, and Y. Tobe, “Recognizing bicycling states with hmm based on accelerometer and magnetometer data,” in *SICE Annual Conference 2011*, 2011, pp. 831–832.

[23] Y. Usami, K. Ishikawa, T. Takayama, M. Yanagisawa, and N. Togawa, “Bicycle behavior recognition using sensors equipped with smartphone,” in *2018 IEEE 8th International Conference on Consumer Electronics-Berlin (ICCE-Berlin)*. IEEE, 2018, pp. 1–6.

[24] W. Gu, Z. Zhou, Y. Zhou, H. Zou, Y. Liu, C. J. Spanos, and L. Zhang, “Bikemate: Bike riding behavior monitoring with smartphones,” in *Proceedings of the 14th EAI International Conference on Mobile and Ubiquitous Systems: Computing, Networking and Services*, ser. MobiQuitous 2017. New York, NY, USA: Association for Computing Machinery, 2017, p. 313–322. [Online]. Available: https://doi.org/10.1145/3144457.3144462

[25] S. Stančin and S. Tomažič, “Smartphone mems accelerometer for cycling–observations.” Ljubljana, 2015.

[26] J. Wu, L. Hong, and V. Frias-Martinez, “Predicting perceived level of cycling safety for cycling trips,” in *Proceedings of the 27th ACM SIGSPATIAL International Conference on Advances in Geographic Information Systems*, ser. SIGSPATIAL ’19. New York, NY, USA: Association for Computing Machinery, 2019, p. 456–459. [Online]. Available: https://doi.org/10.1145/3347146.3359092

[27] S. Verstockt, V. Slavkovikj, P. De Potter, and R. Van de Walle, “Collaborative bike sensing for automatic geographic enrichment: Geoannotation of roadterrain type by multimodal bike sensing,” *IEEE Signal Processing Magazine*, vol. 31, no. 5, pp. 101–111, 2014.

[28] M. Bíl, R. Andrášik, and J. Kubecek, “How comfortable are your cycling tracks? a new method for objective bicycle vibration measurement,” *Transportation Research Part C: Emerging Technologies*, vol. 56, pp. 415 – 425, 07 2015.

[29] M. Y. Alam, H. Anurag, M. S. Imam, S. Saha, M. Saha, S. Nandi, and S. Chakraborty, “Urban safety as a service during bike navigation: My smartphone can monitor my street-lights,” in *2020 IEEE International Conference on Smart Computing (SMARTCOMP)*, 2020, pp. 114–121.

[30] W. Jin, S. Murali, Y. Cho, H. Zhu, T. Li, R. T. Panik, A. Rimu, S. Deb, K. Watkins, X. Yuan, and M. Li, “Cycleguard: A smartphone-based assistive tool for cyclist safety using acoustic ranging,” *Proc. ACM Interact. Mob. Wearable Ubiquitous Technol.*, vol. 5, no. 4, dec 2022. [Online]. Available: https://doi.org/10.1145/3494992

[31] V. M. Puchades, L. Pietrantoni, F. Fraboni, M. D. Angelis, and G. Prati, “Unsafe cycling behaviours and near crashes among italian cyclists,” *International Journal of Injury Control and Safety Promotion*, vol. 25, no. 1, pp. 70–77, 2018, pMID: 28675090. [Online]. Available: https://doi.org/10.1080/17457300.2017.1341931

[32] Physiopedia, “Cycling biomechanics — physiopedia,” 2020, online; accessed 10-November-2021. [Online]. Available: https://www.physio-pedia.com/index.php?title=Cycling_Biomechanics&oldid=238934

[33] C. Stone and M. Hull, “The effect of rider weight on rider-induced loads during common cycling situations,” *Journal of Biomechanics*, vol. 28, no. 4, pp. 365–375, 1995.

[34] R. R. Bini and F. P. Carpes, *Biomechanics of cycling*. Springer, 2014.

[35] E. Bressel and B. Larson, “Bicycle seat designs and their effect on pelvic angle, trunk angle, and comfort,” *Medicine and science in sports and exercise*, vol. 35, pp. 327–32, 02 2003.

[36] E. Bressel and J. Cronin, “Bicycle seat interface pressure: reliability, validity, and influence of hand position and workload,” *Journal of Biomechanics*, vol. 38, no. 6, pp. 1325–1331, 2005. [Online]. Available: https://www.sciencedirect.com/science/article/pii/S0021929004003033

[37] (2016) Pi cap (sku-6515). Bare Conductive. [Online]. Available: https://www.bareconductive.com/products/pi-cap

[38] (2016) Raspberry pi camera (vr-220). Entaniya. [Online]. Available: https://products.entaniya.co.jp/en/products/raspberry-pi-vr-220-camera/

[39] Z. Liu, G. Yao, Q. Zhang, J. Zhang, and X. Zeng, “Wavelet scattering transform for ecg beat classification,” *Computational and Mathematical Methods in Medicine*, vol. 2020, pp. 1–11, 10 2020.

[40] Q. Zhao and L. Zhang, “Ecg feature extraction and classification using wavelet transform and support vector machines,” in *2005 International Conference on Neural Networks and Brain*, vol. 2, 2005, pp. 1089–1092.

[41] K. Juselius, “The cointegrated var model: Methodology and applications,” 2006.

[42] J. Andén and S. Mallat, "Deep scattering spectrum," *IEEE Transactions on Signal Processing*, vol. 62, no. 16, pp. 4114–4128, 2014.

[43] K. Jiokeng, G. Jakllari, and A.-L. Beylot, "Handrate: Heart rate monitoring while simply holding a smartphone," in *2021 IEEE International Conference on Pervasive Computing and Communications (PerCom)*, 2021, pp. 1–11.